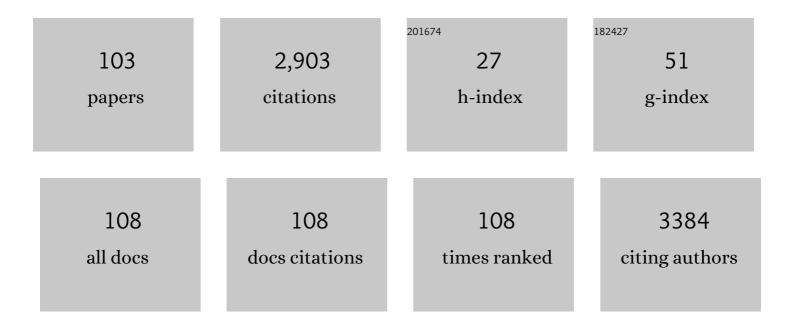
List of Publications by Year in descending order

Source: https://exaly.com/author-pdf/1612741/publications.pdf Version: 2024-02-01



#	Article	IF	CITATIONS
1	Recent advances in the photocatalytic conversion of carbon dioxide to fuels with water and/or hydrogen using solar energy and beyond. Coordination Chemistry Reviews, 2013, 257, 171-186.	18.8	582

Photocatalytic conversion of carbon dioxide into methanol using zinc–copper–M(III) (M=aluminum,) Tj ETQq0 $\begin{array}{c} 0.0 \\ 0.2 \\ 256 \end{array}$ rgBT /Qverlock 10 $\begin{array}{c} 0.0 \\ 256 \end{array}$

3	Photocatalytic conversion of carbon dioxide into methanol using optimized layered double hydroxide catalysts. Catalysis Today, 2012, 185, 263-269.	4.4	119
4	Site Structure and Photocatalytic Role of Sulfur or Nitrogen-Doped Titanium Oxide with Uniform Mesopores under Visible Light. Journal of Physical Chemistry C, 2009, 113, 6706-6718.	3.1	91
5	Tailoring assemblies of plasmonic silver/gold and zinc–gallium layered double hydroxides for photocatalytic conversion of carbon dioxide using UV–visible light. Applied Catalysis A: General, 2015, 504, 238-247.	4.3	70
6	Ligand K-Edge and Metal L-Edge X-ray Absorption Spectroscopy and Density Functional Calculations of Oxomolybdenum Complexes with Thiolate and Related Ligands:Â Implications for Sulfite Oxidase. Journal of the American Chemical Society, 1999, 121, 10035-10046.	13.7	69
7	Dual Photocatalytic Roles of Light: Charge Separation at the Band Gap and Heat via Localized Surface Plasmon Resonance To Convert CO ₂ into CO over Silver–Zirconium Oxide. Journal of the American Chemical Society, 2019, 141, 6292-6301.	13.7	68
8	Photoconversion of carbon dioxide in zinc–copper–gallium layered double hydroxides: The kinetics to hydrogen carbonate and further to CO/methanol. Applied Catalysis B: Environmental, 2014, 144, 561-569.	20.2	58
9	Photo-oxidation of ethanol on mesoporous vanadium–titanium oxide catalysts and the relation to vanadium(IV) and (V) sites. Applied Catalysis A: General, 2007, 325, 276-282.	4.3	56
10	Catalytic conversion of carbon dioxide into dimethyl carbonate using reduced copper-cerium oxide catalysts as low as 353 K and 1.3 MPa and the reaction mechanism. Frontiers in Chemistry, 2013, 1, 8.	3.6	53
11	Photofuel cell comprising titanium oxide and bismuth oxychloride (BiO _{1â^'x} Cl _{1âî'y}) photocatalysts that uses acidic water as a fuel. Journal of Materials Chemistry A, 2015, 3, 8389-8404.	10.3	51
12	Probing the role of nickel dopant in aqueous colloidal ZnS nanocrystals for efficient solar-driven CO2 reduction. Applied Catalysis B: Environmental, 2019, 244, 1013-1020.	20.2	50
13	Photocatalytic conversion of carbon dioxide into methanol in reverse fuel cells with tungsten oxide and layered double hydroxide photocatalysts for solar fuel generation. Catalysis Science and Technology, 2014, 4, 1644-1651.	4.1	49
14	Chiral Self-Dimerization of Vanadium Complexes on a SiO2Surface for Asymmetric Catalytic Coupling of 2-Naphthol:Â Structure, Performance, and Mechanism. Journal of Physical Chemistry B, 2005, 109, 9905-9916.	2.6	46
15	Catalysis on Ruthenium Clusters Supported on CeO2 or Ni-Doped CeO2:  Adsorption Behavior of H2 and Ammonia Synthesis. The Journal of Physical Chemistry, 1996, 100, 9421-9428.	2.9	45
16	Stabilizing Atomically Dispersed Catalytic Sites on Tellurium Nanosheets with Strong Metal–Support Interaction Boosts Photocatalysis. Small, 2020, 16, e2002356.	10.0	45
17	Harnessing self-supported Au nanoparticles on layered double hydroxides comprising Zn and Al for enhanced phenol decomposition under solar light. Applied Catalysis B: Environmental, 2016, 199, 260-271.	20.2	43
18	Ethanol synthesis from carbon dioxide on TiO2-supported [Rh10Se] catalyst. Chemical Communications, 1996, , 389.	4.1	39

#	Article	IF	CITATIONS
19	Molecular sensing techniques for the characterization and design of new ammonia catalysts. Applied Surface Science, 1997, 121-122, 488-491.	6.1	37
20	X-ray Absorption Fine Structure Combined with Fluorescence Spectrometry for Monitoring Trace Amounts of Lead Adsorption in the Environmental Conditions. Analytical Chemistry, 2002, 74, 3819-3823.	6.5	36
21	Study of stereochemical properties of molecular orbitals by Penning ionization electron spectroscopy. Effects of through-space/through-bond interactions on electron distributions. Journal of the American Chemical Society, 1985, 107, 8082-8086.	13.7	34
22	Single Cobalt Atom Anchored Black Phosphorous Nanosheets as an Effective Cocatalyst Promotes Photocatalysis. ChemCatChem, 2020, 12, 3870-3879.	3.7	34
23	Oxidation state of vanadium in amorphous MnV2O6 formed during discharge–charge cycle and the improvement of its synthesis condition. Solid State Ionics, 2006, 177, 1347-1353.	2.7	33
24	Promoting effects of Se on Rh/ZrO2 catalysis for ethene hydroformylation. Journal of Catalysis, 1991, 127, 631-644.	6.2	32
25	CO-breathing structure change and catalysis for oxygenate synthesis from carbon monoxide/hydrogen on supported ruthenium carbido [Ru6C] clusters: structural and chemical controls by interstitial carbido carbon. The Journal of Physical Chemistry, 1994, 98, 594-602.	2.9	32
26	Characterization of Intercalated Iron(III) Nanoparticles and Oxidative Adsorption of Arsenite on Them Monitored by X-ray Absorption Fine Structure Combined with Fluorescence Spectrometry. Journal of Physical Chemistry B, 2005, 109, 3227-3232.	2.6	27
27	X-ray Absorption Fine Structure Combined with X-ray Fluorescence Spectroscopy. Monitoring of Vanadium Sites in Mesoporous Titania, Excited under Visible Light by Selective Detection of Vanadium Kβ _{5,2} Fluorescence. Analytical Chemistry, 2007, 79, 6933-6940.	6.5	27
28	Efficient and Selective Interplay Revealed: CO ₂ Reduction to CO over ZrO ₂ by Light with Further Reduction to Methane over Ni ⁰ by Heat Converted from Light. Angewandte Chemie - International Edition, 2021, 60, 9045-9054.	13.8	27
29	A photofuel cell comprising titanium oxide and silver(<scp>i</scp> /0) photocatalysts for use of acidic water as a fuel. Chemical Communications, 2014, 50, 3067-3070.	4.1	25
30	Ethanol Synthesis from Carbon Dioxide on [Rh10Se]/TiO2Catalyst Characterized by X-Ray Absorption Fine Structure Spectroscopy. Journal of Catalysis, 1998, 175, 236-244.	6.2	24
31	Site-selective XAFS spectroscopy tuned to surface active sites of copper catalysts. Journal of Electron Spectroscopy and Related Phenomena, 2001, 119, 193-199.	1.7	24
32	X-ray Absorption Fine Structure Combined with X-ray Fluorescence Spectrometry. Part 15. Monitoring of Vanadium Site Transformations on Titania and in Mesoporous Titania by Selective Detection of the Vanadium Kα1Fluorescence. Journal of Physical Chemistry B, 2005, 109, 14884-14891.	2.6	24
33	Optimization of an Iron Intercalated Montmorillonite Preparation for the Removal of Arsenic at Low Concentrations. Engineering in Life Sciences, 2007, 7, 52-60.	3.6	24
34	Preferential oxidation of carbon monoxide in hydrogen using zinc oxide photocatalysts promoted and tuned by adsorbed copper ions. Journal of Catalysis, 2012, 287, 190-202.	6.2	24
35	Efficient volcano-type dependence of photocatalytic CO2 conversion into methane using hydrogen at reaction pressures up to 0.80 MPa. Journal of Catalysis, 2017, 345, 39-52.	6.2	24
36	Targeted removal of interfacial adventitious carbon towards directional charge delivery to isolated metal sites for efficient photocatalytic H2 production. Nano Energy, 2020, 76, 105077.	16.0	24

#	Article	IF	CITATIONS
37	Optimized photoreduction of CO2 exclusively into methanol utilizing liberated reaction space in layered double hydroxides comprising zinc, copper, and gallium. Applied Surface Science, 2018, 447, 687-696.	6.1	23
38	Efficient photocatalytic CO ₂ reduction mediated by transitional metal borides: metal site-dependent activity and selectivity. Journal of Materials Chemistry A, 2020, 8, 21833-21841.	10.3	23
39	X-ray Absorption Fine Structure Combined with X-ray Fluorescence Spectrometry. Improvement of Spectral Resolution at the Absorption Edges of 9â^'29 keV. Analytical Chemistry, 2005, 77, 6969-6975.	6.5	22
40	Recent Advances (2012–2015) in the Photocatalytic Conversion of Carbon Dioxide to Fuels Using Solar Energy: Feasibilty for a New Energy. ACS Symposium Series, 2015, , 1-46.	0.5	20
41	Nanoparticles of Amorphous Ruthenium Sulfide Easily Obtainable from a TiO2-Supported Hexanuclear Cluster Complex [Ru6C(CO)16]2â^': A Highly Active Catalyst for the Reduction of SO2 with H2. Chemistry - A European Journal, 2002, 8, 3260.	3.3	19
42	Adsorbed Hydrogen Effect on the Adsorption and Reactivity of N2Molecules on Ru/MgO and Ru–Cs+/MgO: Hydrogen Dipole Effect Enhanced by Doped Cs+. Bulletin of the Chemical Society of Japan, 1994, 67, 3191-3200.	3.2	18
43	Site-Selective X-Ray Absorption Fine Structure (XAFS) Spectroscopy. (1) Design of Fluorescence Spectrometer and Emission Spectra. Bulletin of the Chemical Society of Japan, 2000, 73, 2017-2023.	3.2	18
44	Site-Selective X-Ray Absorption Fine Structure (XAFS) Spectroscopy (2). XAFS Spectra Tuned to Surface Active Sites of Cu/ZnO and Cr/SiO2Catalysts. Bulletin of the Chemical Society of Japan, 2000, 73, 1581-1587.	3.2	18
45	Recent Advances in the Preferential Thermal-/Photo-Oxidation of Carbon Monoxide: Noble Versus Inexpensive Metals and Their Reaction Mechanisms. Catalysis Surveys From Asia, 2016, 20, 141-166.	2.6	18
46	ls water more reactive than H2 in photocatalytic CO2 conversion into fuels using semiconductor catalysts under high reaction pressures?. Journal of Catalysis, 2017, 352, 452-465.	6.2	17
47	Monitoring of Trace Amounts of Lead on an Adsorbent by X-ray Absorption Spectroscopy Combined with a Fluorescence Spectrometer. Journal of Physical Chemistry B, 2002, 106, 1518-1520.	2.6	16
48	Structure of low concentrations of vanadium on TiO2 determined by XANES and ab initio calculations. Chemical Communications, 2002, , 2402-2403.	4.1	16
49	Selective Butanol Synthesis over Rhodiumâ^'Molybdenum Catalysts Supported in Ordered Mesoporous Silica. Journal of Physical Chemistry C, 2007, 111, 10073-10081.	3.1	16
50	Promoting effects of Se on Rh/SiO2 catalysis for ethene hydroformylation. Journal of Catalysis, 1991, 132, 566-570.	6.2	15
51	Rapid and sensitive XAFS using a tunable X-ray undulator. Journal of Synchrotron Radiation, 1999, 6, 155-157.	2.4	15
52	Carbon monoxide-breathing ruthenium carbido clusters on magnesium oxide (MgO) in CO/H2 reaction conditions. Journal of the American Chemical Society, 1993, 115, 6462-6463.	13.7	14
53	Promoted Catalysis by Supported [Ru6N] Clusters in N2 and/or H2: Structural and Chemical Controls. The Journal of Physical Chemistry, 1995, 99, 10346-10353.	2.9	14
54	Preparation of [Ru6N] Clusters on MgO, K+/MgO, Cs+/MgO, and Al2O3 and the Reactivities with H2 and N2. The Journal of Physical Chemistry, 1995, 99, 10336-10345.	2.9	13

#	Article	IF	CITATIONS
55	Selective Photoconversion of Carbon Dioxide into Methanol Using Layered Double Hydroxides at 0.40â€MPa. Energy Technology, 2017, 5, 892-900.	3.8	13
56	Selenium-doped hexarhodium carbonyl clusters on magnesia: structures and promoting effects in ethene hydroformylation. The Journal of Physical Chemistry, 1992, 96, 10942-10948.	2.9	12
57	Selective synthesis of oxygenates in the CO–H2reaction on supported ruthenium carbido-cluster catalysts. Journal of the Chemical Society Chemical Communications, 1992, , 1395-1396.	2.0	11
58	Simultaneous Removal of NO and N2O over Pd-ZSM-5 Catalysts and FT-IR Observations of their Decomposition Routes to N2. Bulletin of the Chemical Society of Japan, 2001, 74, 1499-1505.	3.2	11
59	Synthesis of Clay—Cerium Hydroxide Conjugates for the Adsorption of Arsenic. Adsorption Science and Technology, 2005, 23, 607-618.	3.2	11
60	Rapid and sensitive XAFS using a tunable X-ray undulator at BL10XU of SPring-8. Journal of Synchrotron Radiation, 2000, 7, 89-94.	2.4	10
61	Specific Oxidative Dehydrogenation Reaction Mechanism over Vanadium(IV/III) Sites in TiO2 with Uniform Mesopores under Visible Light. Bulletin of the Chemical Society of Japan, 2008, 81, 1241-1249.	3.2	10
62	Arsenic Removal from Dilute Solutions by High Surface Area Mesoporous Iron Oxyhydroxide. Water, Air and Soil Pollution, 2009, 9, 203-211.	0.8	10
63	Preferential Photooxidation of CO in Hydrogen across the Crystalline Face Boundary over Spheroidal ZnO Promoted by Cu Ions. Journal of Physical Chemistry C, 2015, 119, 21585-21598.	3.1	10
64	Nitrous oxide decomposition active site on Ni–MgO catalysts characterized by X-ray absorption fine structure spectroscopy. Chemical Communications, 2000, , 1053-1054.	4.1	9
65	Photocatalytic Conversion of Carbon Dioxide Using Zn–Cu–Ga Layered Double Hydroxides Assembled with Cu Phthalocyanine: Cu in Contact with Gaseous Reactant is Needed for Methanol Generation. Oil and Gas Science and Technology, 2015, 70, 841-852.	1.4	9
66	Direct Detection of Redox Reactions of Sulfur-containing Compounds on Ferrite Nanoparticle (FP) Surface. Chemistry Letters, 2006, 35, 974-975.	1.3	8
67	Synthesis and Site Structure of a Replica Platinumâ^Carbon Composite Formed Utilizing Ordered Mesopores of Aluminum-MCM-41 for Catalysis in Fuel Cells. Journal of Physical Chemistry C, 2010, 114, 1260-1267.	3.1	8
68	Anchoring and reactivation of single-site Co–porphyrin over TiO2 for the efficient photocatalytic CO2 reduction. Journal of Catalysis, 2022, 413, 588-602.	6.2	8
69	Creation of micro and mesoporous Felll materials utilizing organic template followed by carboxylates exchange for the low concentrations of arsenite removal. Microporous and Mesoporous Materials, 2006, 94, 243-253.	4.4	7
70	Monitoring of Sulfur Sites Doped in/on Titanium Oxide to Enable Photocatalysis under Visible Light Using S K-edge XANES. Chemistry Letters, 2009, 38, 912-913.	1.3	7
71	Polymer electrolyte fuel cell supplied with carbon dioxide. Can be the reductant water instead of hydrogen?. Applied Catalysis B: Environmental, 2012, 117-118, 317-320.	20.2	7
72	Promoting effects of Se on the activity and selectivity of Rh–ZrO2catalyst for ethene hydroformylation. Journal of the Chemical Society Chemical Communications, 1988, , 1327-1328.	2.0	6

#	Article	IF	CITATIONS
73	Selective carbonyl insertion and ethene hydroformylation on a [Ru6C(CO)16Me]––SiO2catalyst. Journal of the Chemical Society Dalton Transactions, 1993, , 3667-3673.	1.1	6
74	Nitric Oxide Reduction by Carbon Monoxide over Supported Hexaruthenium Cluster Catalysts. 1. The Active Site Structure That Depends on Supporting Metal Oxide and Catalytic Reaction Conditions. Journal of Physical Chemistry B, 2003, 107, 9022-9028.	2.6	6
75	Sulfur K-edge extended X-ray absorption fine structure spectroscopy of homoleptic thiolato complexes with Zn(II) and Cd(II). Journal of Inorganic Biochemistry, 2006, 100, 239-249.	3.5	6
76	State-sensitive monitoring of gold nanoparticle sites on titania and the interaction of the positive Au site with O2 by Au Lα1-selecting X-ray absorption fine structure. Inorganica Chimica Acta, 2008, 361, 1149-1156.	2.4	6
77	Binary metal (Ti, Cu) oxyhydroxy–organic (terephthalate) framework: An interface model nanocatalyst for hydrogen purification. Journal of Catalysis, 2015, 332, 1-12.	6.2	6
78	Why Is Water More Reactive Than Hydrogen in Photocatalytic CO2 Conversion at Higher Pressures? Elucidation by Means of X-Ray Absorption Fine Structure and Gas Chromatography–Mass Spectrometry. Frontiers in Chemistry, 2018, 6, 408.	3.6	6
79	Efficient and Selective Interplay Revealed: CO ₂ Reduction to CO over ZrO ₂ by Light with Further Reduction to Methane over Ni ⁰ by Heat Converted from Light. Angewandte Chemie, 2021, 133, 9127-9136.	2.0	6
80	Dual origins of photocatalysis: Light-induced band-gap excitation of zirconium oxide and ambient heat activation of gold to enable 13CO2 photoreduction/conversion. Catalysis Today, 2020, 356, 544-556.	4.4	6
81	Methylruthenium carbidocarbonyl clusters supported on inorganic oxides: characterization and selective acetaldehyde formation. Journal of the Chemical Society Dalton Transactions, 1992, , 2287.	1.1	5
82	Site-selective XAFS spectroscopy tuned to surface active sites of Cu/ZnO and Cr/SiO2catalysts. Journal of Synchrotron Radiation, 2001, 8, 605-607.	2.4	5
83	0.6–3.0 wt% of Vanadium on/in Titania Monitored by X-ray Absorption Fine Structure Combined with Fluorescence Spectrometry. Chemistry Letters, 2002, 31, 1154-1155.	1.3	5
84	Cluster-derived Ir–Sn/SiO2 catalysts for the catalytic dehydrogenation of propane: a spectroscopic study. Dalton Transactions, 2013, 42, 12714.	3.3	5
85	Solar Cell with Photocatalyst Layers on Both the Anode and Cathode Providing an Electromotive Force of Two Volts per Cell. ACS Sustainable Chemistry and Engineering, 2018, 6, 11892-11903.	6.7	5
86	Local Silver Site Temperature Critically Reflected Partial and Complete Photooxidation of Ethanol Using Ag–TiO ₂ as Revealed by Extended X-ray Absorption Fine Structure Debye–Waller Factor. Journal of Physical Chemistry C, 2021, 125, 14689-14701.	3.1	5
87	Recyclable PhotoFuel Cell for Use of Acidic Water as a Medium. Oil and Gas Science and Technology, 2015, 70, 853-862.	1.4	5
88	Monitoring Trace Amounts of Lead and Arsenic Adsorption by Xray Absorption Fine Structure Combined with Fluorescence Spectrometry. Physica Scripta, 2005, , 933.	2.5	4
89	Photo-oxidation over mesoporous V-TiO2 catalyst under visible light monitored by vanadium Kβ5,2-selecting XANES spectroscopy. Materials Letters, 2008, 62, 861-864.	2.6	4
90	X-ray evaluation of the boundary between polymer electrolyte and platinum and carbon functionalization to conduct protons in polymer electrolyte fuel cells. Journal of Power Sources, 2014, 258, 83-88.	7.8	3

#	Article	IF	CITATIONS
91	A solar cell for maximizing voltage up to the level difference of two photocatalysts: optimization and clarification of the electron pathway. RSC Advances, 2017, 7, 19996-20006.	3.6	3
92	Polarizability and Catalytic Activity Determine Good Titanium Oxide Crystals but Not Homogeneity in Solar Cells Using Photocatalysts on Both Electrodes. ACS Sustainable Chemistry and Engineering, 2020, 8, 1406-1416.	6.7	3
93	Optimization of high voltage-type solar cell comprising thin TiO2 on anode and thin Ag–TiO2 photocatalysts on cathode. Solar Energy, 2020, 208, 604-611.	6.1	3
94	Promoting effect and hydrogen spillover in supported SeRh6-cluster catalysts. Studies in Surface Science and Catalysis, 1993, 77, 241-246.	1.5	2
95	X-ray absorption fine structure combined with X-ray fluorescence spectrometry. Materials Letters, 2007, 61, 3833-3836.	2.6	2
96	New Supported [Ru6N] Clusters as a Potential Transition Metal Nitride Catalyst. Chemistry Letters, 1995, 24, 137-138.	1.3	1
97	Characterization of Active Site on Cobalt-Magnesium Oxide by X-Ray Absorption Fine Structure Spectroscopy. Chemistry Letters, 1998, 27, 727-728.	1.3	1
98	Oxygen atom radical formation on the sol-gel molybdenum-silica catalysts characterized by X-ray absorption fine structure spectroscopy. Studies in Surface Science and Catalysis, 2000, 130, 3201-3206.	1.5	1
99	State-Sensitive Monitoring of Active and Promoter Sites. Applications to Au/Titania and Pt-Sn/Silica Catalysts by XAFS Combined with X-Ray Fluorescence Spectrometry. AIP Conference Proceedings, 2007, ,	0.4	1
100	Monitoring of Photochemical Self-assembly of [Mo7O24]6â^' to {Mo142}-blue Nanoring by Using Mo K-edge XAFS. Chemistry Letters, 2010, 39, 132-133.	1.3	1
101	Photocatalytic Conversion of Carbon Dioxide into Fuels Using Layered Double Hydroxides Coupled with Hydrogen or Water. , 2013, , 589-602.		1
102	Supported ruthenium carbido-cluster catalysts for the catalytic removal of nitrogen monoxide and sulfur dioxide: the preparation process monitored by sulfur K-edge X-ray absorption near-edge structure. Studies in Surface Science and Catalysis, 2000, 143, 361-368.	1.5	0
103	32 X-ray absorption fine structure utilizing a fluorescence spectrometer: Site selective structure determination of environmental catalysts and adsorbents. Studies in Surface Science and Catalysis, 2003, 145, 177-180.	1.5	Ο